Bioorganic & Medicinal Chemistry Letters 26 (2016) 4310–4317

Contents lists available at ScienceDirect

Bioorganic & Medicinal Chemistry Letters

journal homepage: www.elsevier.com/locate/bmcl

Gold catalyzed double condensation reaction: Synthesis, antimicrobial and cytotoxicity of spirooxindole derivatives

K. Parthasarathy [a], Chandrasekar Praveen [b,*], J. C. Jeyaveeran [c], A. A. M. Prince [c]

[a] Department of Chemistry, Siddha Central Research Institute, Central Council for Research in Siddha, Arumbakkam, Chennai 600106, Tamil Nadu, India
[b] Functional Materials Division, CSIR-Central Electrochemical Research Institute, Karaikudi 630003, Tamil Nadu, India
[c] Department of Chemistry, Ramakrishna Mission Vivekananda College, Mylapore, Chennai 600004, Tamil Nadu, India

ARTICLE INFO

Article history:
Received 23 May 2016
Revised 7 July 2016
Accepted 18 July 2016
Available online 19 July 2016

Keywords:
Microwave chemistry
Gold catalysis
Spirooxindoles
Biological activity
Molecular docking

ABSTRACT

Microwave assisted synthesis of spirooxindoles via tandem double condensation between isatins and 4-hydroxycoumarin under gold catalysis is reported. The reaction is practical to perform, since the products can be isolated by simple filtration without requiring tedious column chromatography. The scope of this chemistry is exemplified by preparing structurally diverse spirooxindoles (22 examples) in excellent yields. Antimicrobial evaluation of the synthesized compounds revealed that three compounds (**3a**, **3f** and **3s**) exhibited significant MIC values in comparison to the standard drugs. Molecular docking studies of these compounds with AmpC-β-lactamase receptor revealed that **3a** exhibited minimum binding energy (−117.819 kcal/mol) indicating its strong affinity towards amino acid residues via strong hydrogen bond interaction. All compounds were also evaluated for their in vitro cytotoxicity against COLO320 cancer cells. Biological assay and molecular docking studies demonstrated that **3g** is the most active compound in terms of its low IC_{50} value (50.0 μM) and least free energy of binding (−8.99 kcal/mol) towards CHK1 receptor, respectively.

Spirooxindoles have received paramount importance, because of their prevalence as substructure in numerous bioactive agents and natural products.[1] On the other hand, 4-hydroxycoumarin is a structural component present in various pharmaceuticals/clinical drugs such as warfarin, phenprocoumon, acenocoumarol, tioclomarol and brodifacoum (Fig. 1).[2] Inspired by their pharmacological properties and synthetic feasibility, it was thought worthwhile to fuse both these scaffolds as a single molecular entity in view of enhanced biological activity. Towards this end, we intended a simple and straightforward synthesis of hybrid-spirooxindoles via bis-condensation between isatin and 4-hydroxycoumarin. Only limited reports were documented for this type of transformations though with narrow substrate scope (*N*-unsubstituted). For example, a substituent at the isatinyl nitrogen was not reported in the previously reported *p*-TSA and I_2 catalyzed protocols.[3] In another finding, the solvent-induced synthesis of similar compounds under dry conditions was disclosed albeit with less product selectivity.[4] In order to circumvent these limitations coupled with our research endeavors in homogeneous gold catalysis,[5] we sought to investigate whether it would be possible to accomplish the aforementioned transformation under gold catalysis. To this end, we herein report a practical and efficient gold(III)-catalyzed double condensation reaction between isatin and 4-hydroxycoumarin under microwave condition. The resulting spirooxindole[pyrano-bis-2*H*-l-benzopyrans] were evaluated for their antimicrobial and cytotoxic properties. Additionally, molecular docking of most active compounds with appropriate receptors was performed and all these results were disclosed in this Letter.

Based on our previous experience with gold catalysis,[5] we initially screened few Au(I) and Au(III) catalysts for the prototype reaction between isatin (1.0 mmol) and 4-hydroxycoumarin (2.0 mmol) at 80 °C (Scheme 1, Table 1). In this effort, we found that AuCl, Ph_3PAuCl and $AuCl_3$ afforded poor yield of product **3a** in both dichloroethane and ethanol (entries 1–5). Among the triflimide complexes screened $Ph_3PAuNTf_2$ gave slightly better yield over *t*-$Bu_3PAuNTf_2$ (entries 6 and 7). The use of alkali gold salts such as $KAuCl_4$ and $NaAuCl_4{\cdot}2H_2O$ enhanced the yield of **3a** to 57% and 59%, respectively (entries 8 and 9). Since, $NaAuCl_4{\cdot}2H_2O$ is relatively cheaper than $KAuCl_4$, our further investigation focused only on the use of the sodium salt. Reducing the catalytic amount of $NaAuCl_4{\cdot}2H_2O$ from 5 to 2 mol % resulted in no appreciable change in yield (entry 10) and thus evaluated for subsequent screening. A drastically reduced yield was observed, when the reaction was performed at room temperature suggesting the necessity of elevated temperature in this transformation (entry

* Corresponding author.
E-mail address: chandrasekar.praveen@gmail.com (C. Praveen).

http://dx.doi.org/10.1016/j.bmcl.2016.07.036
0960-894X/

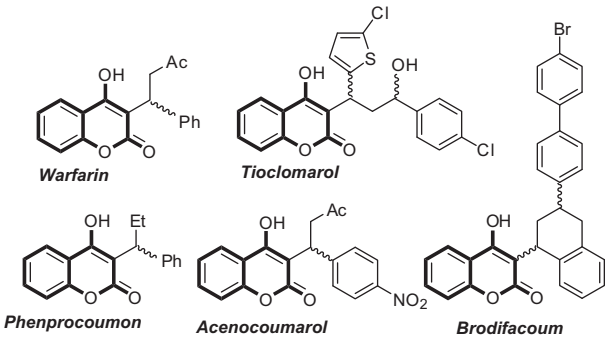

Figure 1. Pharmaceuticals containing of 4-hydroxycoumarin scaffold.

11). Through this observation, we rationalized that the reaction rate could be escalated by microwave irradiation instead of conventional heating. To our delight, microwave irradiation of model reaction at 25 °C afforded 79% yield of **3a** (entry 12). A slight increase of temperature to 40 °C resulted in an excellent yield of 92% (entry 13). When the solvent was changed from ethanol to dichloroethane more or less same yield of **3a** (90%) was obtained (entry 14). A blank reaction led to no product formation confirmed the role of $NaAuCl_4{\cdot}2H_2O$ as catalytic species (entry 15). In view of the fact that, ethanol has a loss tangent (tan δ value) of 0.941 in microwave promoted reactions and dielectric constant (ε') of 24.6; we preferred it over dichloroethane for further studies.[6] From the screening data, it is quite obvious that 2 mol % of $NaAuCl_4{\cdot}2H_2O$ in ethanol at 40 °C under an irradiation of 200 W was effective for the desired transformation (entry 13). Hence, this reaction condition was employed for a wide range of substrates toward the preparation of structurally diverse spirooxindoles.

Initially, we prepared a series of *N*-substituted isatins required for our study by several closely related N-alkylation procedures in synthetically good yields.[7] In order to fully examine the scope of our chemistry, various isatins and 4-hydroxycoumarin were tested under our optimized conditions (Scheme 2, Table 2). The reaction appears to be general and works well regardless of the electronic nature of the peripheral substituent (R and R^1) on the isatin moiety and afforded good to excellent yield of products **3a**–**3u** (Table 2). This uniformity in yields irrespective of the electronic nature of the substituent can be explained by looking at the increased electrophilicity at the C3-carbonyl of isatin via Au(III) activation, thus facilitating the nucleophilic addition of 4-hydroxycoumarin. The protocol is amenable to substrates containing peripheral substituent at all positions (R and R^1), whereas a substitution at the isatinyl nitrogen was not reported in other catalytic protocols.[3] One of the significant advantages of the current methodology is its scope towards substrate possessing C–C multiple bonds (**3q** and **3r**), since it is well known that, Au(III)-catalyst activates unsaturated bonds via typical π-activation chemistry.[8]

The utility of this chemistry was further manifested by its applicability to afford product with propargyl tether **3r** without observing any allene-isomerization.[9] Interestingly, our Au(III)-catalyzed spirooxindole formation strategy is not only limited to mono-systems but also can be extended to bis-system. As illustrated in Scheme 3, we have been able to apply this chemistry to the synthesis of complex bis-isatinyl system. Thus, treatment of 1,1′-(propane-1,3-diyl)bis-isatin **1v** (1.0 mmol) with 4-hydroxycoumarin (4.0 mmol) under our standard conditions generated the corresponding bis-spiro skeleton **3v** in 81% yield.

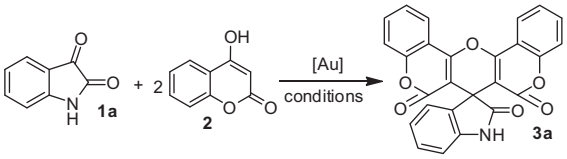

Scheme 1. Proposed synthesis of target **3a**.

In another study, we subjected *N*-methylisatin (1.0 mmol) with 4-hydroxy-6-methyl-2*H*-pyran-2-one (2.0 mmol) under our standard conditions in view of obtaining the bis-condensation product **3w** (Scheme 4). In contrast to our expectation, the product **4w** was obtained as the sole product in low yield. This observation was in sharp agreement with results obtained using $Rh(cod)_2BF_4$ as catalyst by Stephenson et al.[10] Nevertheless, we were able to achieve excellent diastereoselectivity in this transformation (dr = 95:05 vs 5:1).

The structure of all products was confirmed by spectral data (FTIR, ^{1}H NMR, ^{13}C NMR and MS) and elemental analyses. As a representative example, the IR spectrum of compound **3a** showed a broad peak at 3411 cm^{-1} and a sharp peak at 1708 cm^{-1}, which corresponds respectively to the –NH and carbonyl functionalities of the oxindole core. Sharp stretching bands at 1732 and 1662 cm^{-1} suggested the presence of carbonyl group characteristic of the δ-lactone ring. In ^{1}H NMR spectrum, twelve protons resonated at aryl region (δ_H 6.84–8.48 ppm) and a broad singlet at δ_H 10.85 ppm corresponds to –NH proton (D_2O exchangeable) of the oxindole moiety. The ^{13}C NMR spectrum of **3a** recorded in DMSO-d_6 showed seventeen carbons. A less intense peak at δc 46.5 ppm indicates the presence of a quaternary carbon in the aliphatic region (spiro carbon). Two peaks at δc 157.9 and 176.4 ppm corresponds to the carbonyl carbon of the coumarin and oxindole, respectively. This observation was supported by DEPT-135 and 2D chemical shift correlation experiments (see Supplementary data). Finally, HRMS data showed a peak at $m/z_{(obs.)}$ = 458.0641 corresponds to $[M+Na]^+$, where M is the molecular mass of **3a** is in well agreement with the expected $m/z_{(expd.)}$ = 458.0635. All these experimental data unambiguously confirmed the structure of compound **3a**.

Based on the observed results, a tentative mechanism was proposed (Scheme 5) for the formation of representative compound **3a**. According to which, 4-hydroxycoumarin **2** undergoes nucleophilic addition at the C3 carbon of the [Au] activated isatin to form intermediate **I**. Dehydration of intermediate **I** results in the formation of intermediate **II**. The Lewis acidic [Au] again enters the catalytic cycle by interacting with the carbonyl oxygen of **II** and drives the addition of another molecule of 4-hydroxycoumarin **2**

Table 1
Screening of Lewis acids[a]

Entry	Catalyst	mol %	Solvent	Temp (°C)	Time (min)	Yield[b] (%)
1	AuCl	5	$(CH_2Cl)_2$	80	60	25
2	AuCl	5	EtOH	80	60	26
3	Ph_3PAuCl	5	EtOH	80	60	22
4	$AuCl_3$	5	$(CH_2Cl)_2$	80	60	15
5	$AuCl_3$	5	EtOH	80	60	18
6	$Ph_3PAuNTf_2$	5	EtOH	80	60	39
7	t-$Bu_3PAuNTf_2$	5	EtOH	80	60	28
8	$KAuCl_4$	5	EtOH	80	60	57
9	$NaAuCl_4{\cdot}2H_2O$	5	EtOH	80	60	59
10	$NaAuCl_4{\cdot}2H_2O$	2	EtOH	80	60	58
11	$NaAuCl_4{\cdot}2H_2O$	2	EtOH	25	120	10
12	$NaAuCl_4{\cdot}2H_2O$	2	EtOH	25	60	79[c]
13	$NaAuCl_4{\cdot}2H_2O$	**2**	**EtOH**	**40**	**15**	**92[c]**
14	$NaAuCl_4{\cdot}2H_2O$	2	$(CH_2Cl)_2$	40	15	90[c]

[a] All reactions were performed using 1.0 mmol of isatin and 2.0 mmol of 4-hydroxycoumarin.
[b] Isolated yield after filteration.
[c] Reaction was performed under microwave irradiation with a power level of 200 W.

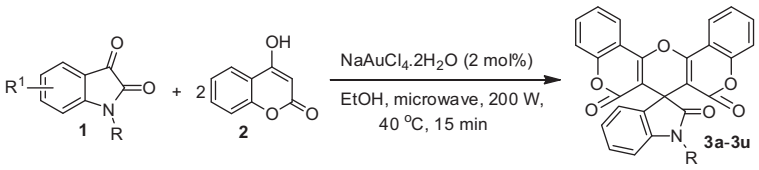

Scheme 2. Synthesis of targeted spirooxindoles **3a**–**3u**.

Table 2
Synthesis of **3a**–**3u** under optimized conditions

Entry	R	R^1	Product[a]	Yield[b] (%)
1	H	H	**3a**	92
2	H	4-Cl	**3b**	96
3	H	5-Me	**3c**	93
4	H	5-F	**3d**	92
5	H	5-Cl	**3e**	89
6	H	5-Br	**3f**	88
7	H	5-NO_2	**3g**	86
8	H	6-Cl	**3h**	91
9	H	7-F	**3i**	95
10	H	7-Cl	**3j**	90
11	Me	H	**3k**	95
12	Et	H	**3l**	95
13	*n*-Pr	H	**3m**	94
14	*n*-Bu	H	**3n**	95
15	Pentyl	H	**3o**	91
16	Hexyl	H	**3p**	90
17	Allyl	H	**3q**	93
18	Propargyl	H	**3r**	91
19	Bn	H	**3s**	94
20	2-F-Bn	H	**3t**	92
21	Me	5-F	**3u**	89

[a] All products were characterized by IR, ^{1}H NMR ^{13}C NMR & mass.
[b] Isolated yield after filtration.

leading to **III**. The later upon intramolecular cyclization results in intermediate **IV** and subsequent dehydration affords the product **3a**.

In continuation of our on-going project on bio-active heterocycles,[11] all the prepared compounds (**3a**–**3u**) were tested for their antibacterial activity against nine bacterial strains (*Staphylococcus epidermidis*, *Salmonella typhimurium*, *Klebsiella pneumonia*, *Bacillus subtilis*, *Shigella flexneri*, *Micrococcus luteus*, *Enterobacter aerogenes*, *Staphylococcus aureus* and *Staphylococcus aureus* MRSA) and antifungal activity against two fungal strains (*Candida albicans*, *Malassezia pachydermatis*) using disc diffusion method.[12] Analysis of the screening results revealed that most of the compounds exhibited comparable antibacterial and antifungal activities against reference drugs (Table 3).

Out of the 22 compounds screened, 9 compounds (**3a**, **3e**, **3f**, **3k**, **3l**, **3p**, **3r**, **3s** and **3t**) emerged as the most active against all antimicrobial strains. It is noteworthy to mention that these compounds exhibited greater zone of inhibition than the standard drugs. Other compounds (**3b**–**3d**, **3g**–**3j**, **3m**–**3o**, **3q** and **3u**) showed moderate activities against the tested strains as indicated by their reduced zone of inhibition values. Based on these encouraging results, the most active compounds (**3a**, **3e**, **3f**, **3k**, **3l**, **3p**, **3r**, **3s** and **3t**) were assessed in terms of minimum inhibitory concentration (MIC) by standard reference methods (Table 4).[13] MIC is defined as the maximum dilution of the test compound that inhibits the growth of the microorganism. The selected compounds were dissolved in DMSO to prepare a series of descending concentration (1000 μM, 500 μM, 250 μM, 125 μM, 62.5 μM, 31.25 μM, 15.62 μM and 7.81 μM). These solutions were then diluted to give serial two-fold dilutions and were added to each medium in 96 well plates. An inoculum of 100 μL from each well was inoculated. The references, ketoconazole for fungi and streptomycin for bacteria were included in the assays as positive controls. For fungi, the plates were incubated for 48 to 72 h at 28 °C and for bacteria the plates were incubated for 24 h at 37 °C. The MIC for fungi was defined as the lowest concentration showing no visible fungal growth after the incubation time. 5 μL of tested broth was placed on the sterile MHA plates for bacteria and incubated at respective temperature. The MIC for bacteria was determined as the lowest concentration of the compound inhibiting the visual growth of the test cultures on the agar plate. The MIC values of active compounds against bacteria and fungi are given in Table 4, which revealed that among the nine compounds tested, compound **3a** devoid of any substitution showed activity against *Enterobacter aerogenes* (31.25 μM) and *Staphylococcus aureus* MRSA (7.81 μM). Compound **3f** possessing bromo substituent at the C5-carbon of the oxindole core exhibited activity against *Staphylococcus epidermidis* (31.25 μM) and *Staphylococcus aureus* (7.81 μM). Compound **3s** possessing *N*-benzyl substituent showed activity against *Staphylococcus epidermidis* (31.25 μM), *Staphylococcus aureus* (7.81 μM) and *Candida albicans* (31.25 μM). Whereas, other compounds **3e**, **3k**, **3l**, **3p**, **3r** and **3t** displayed insignificant MIC values against all antimicrobial strains.

In the present study all compounds (**3a**–**3u**) were tested for their cytotoxic potential against colorectal adenocarcinoma cell lines (COLO320) by MTT assay.[14] The cytotoxic results were compared with reference drug cyclophosphamide which showed 90% inhibition at a concentration of 156 μM. The tested compounds exhibited maximum cytotoxicity against COLO320 cells at a

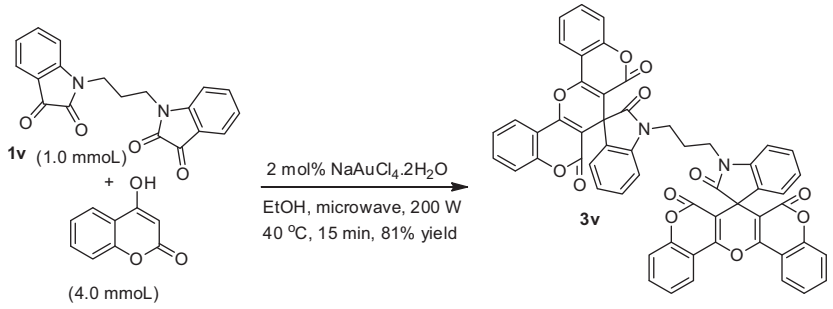

Scheme 3. Synthesis of bis-spiroxindole system **3v**.

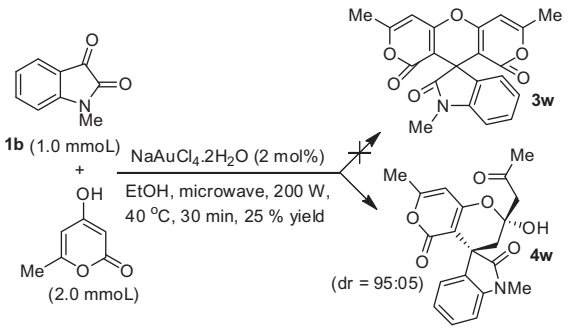

Scheme 4. Au(III)-catalyzed formation of compound **2b**.

concentration of 100 to 50 μM. All concentrations used in the experiment could decrease the cell viability significantly ($P < 0.05$) in a concentration-dependent manner. Cytotoxicity of each sample was expressed as IC_{50} value. The IC_{50} value is the concentration of test sample that causes 50% inhibition of cell growth averaged from three replicate experiments (Table 5). Attempts to understand the SAR of the spirooxindoles started with the substitution at the C5 position, which revealed that replacement of C5-F (**3d**, IC_{50} = >100 μM) by C5-Cl (**3e**, IC_{50} > 55.5 μM) or C5-Br (**3f**, IC_{50} = 52.7 μM) did increased the potency to a great extent. Similar trend was observed, when C5-Br (**3f**, IC_{50} = 52.7 μM) was replaced by C5-NO_2 (**3g**, IC_{50} = 50.0 μM) and resulted in an escalation of activity. The increase in activity with respect to different substitution could be attributed to the increase in size (F < Cl < Br < NO_2) of the respective substituent. Halo substitution other than C5 position, such as C4 (**3b**), C6 (**3h**) and C7 (**3i** and **3j**) completely failed to show appreciable cytotoxicity as evidenced by their higher IC_{50} values (>100 μM). These comparisons clearly suggested that the presence of C5-substituent is essential in order to realize good inhibitory potency. It is apparent from the data presented in Table 5, that with the every increase in the number of –CH_2 spacer, the inhibitory potency also increased. This drift was observed in analogues containing NH (**3a**, IC_{50} = 57.2 μM), NMe (**3k**, IC_{50} = 54.5 μM), NEt (**3l**, IC_{50} = 53.9 μM) and NPr (**3m**, IC_{50} = 51.1 μM), which showed the activity increased in the order NPr > NEt > NMe > NH. Conversely, a completely opposite trend was observed when the carbon chain goes beyond the three methylene spacer **3m**. For example, a slightly reduced potency was observed for the NBu analogue (**3n**, IC_{50} = 51.8 μM) when compared to the NPr analogue (**3m**, IC_{50} = 51.1 μM). Higher congeners such as the *N*-pentyl (**3o**, IC_{50} >100 μM), and *N*-hexyl (**3p**, IC_{50} >100 μM) exhibited a drastically decreased cytotoxicity. Among the unsaturated systems, compound with a propargyl group (**3r**, IC_{50} >100 μM) demonstrated significant cytotoxicity against its allyl counterpart (**3q**, IC_{50} = 54.2 μM). Assessment of the aryl groups revealed that compound with 2-fluorobenzyl substituent (**3t**, IC_{50} = 51.8 μM) exhibited an elevated cytotoxicity than those containing the benzyl (**3s**, IC_{50} = 53.1 μM). This slight enhancement in activity is mainly attributed to the differences in size and electronegativity offered by the fluorine atom. However, when the fluorine atom was located on the C5-position (**3u**, IC_{50} = 55.3 μM), it renders the molecule less active than its unsubstituted counterpart (**3k**, IC_{50} = 54.5 μM). Analysis of the combined results as depicted in Table 3, indicates that compound with a –NO_2 group (**3g**, IC_{50} = 50.0 μM) positioned at the C5 of the oxindole core emerged as the most active. Compound with *N*-propyl substituent (**3m**, IC_{50} = 51.1 μM) was found to be the second most active compound. Compounds possessing butyl (**3n**, IC_{50} = 51.8 μM) and 2-fluorobenzyl groups (**3t**, IC_{50} = 51.8 μM) respectively showed same but significant inhibitory potencies and emerged as the third most active among the screening hits.

The precise prediction of ligand–protein complexes is of fundamental importance in modern structure based drug design.[15] The ligand matching and the corresponding docking score could confirm the binding efficiency of each molecule at the binding site. To this end, selected ligands were docked into AmpC-β-lactamase and Checkpoint kinase 1 (CHK) receptors to evaluate the antimicrobial and cytotoxic activities, respectively. Docking of ligands to the receptor was assessed using Moldock scoring function for antimicrobial and AUTODOCK for cytotoxicity and all the results were discussed in the following sections. The level of antimicrobial activity was studied computationally by Molegro Virtual Docker (MVD) by automated docking of the most active compounds **3a**, **3f** and **3s** to the binding site of AmpC-β-lactamase. The MolDock scoring function used by MVD is derived from the piecewise linear potential (PLP) scoring functions. The MolDock further improves these scoring functions with new hydrogen bonding term and new charge schemes. The ligand matching and the corresponding scoring could confirm the binding efficiency of each molecule at the binding site which are evaluated and ranked according to Moldock scoring function.[16] Experimentally, X-ray crystal structure of AmpC-β-lactamase from *Escherichia coli* was retrieved from Protein Data Bank (PDB) database-1KE4.[17] Computationally, Molegro virtual docker was used to predict the potential binding site on AmpC-β-lactamase. Based on the cavities detected, the most active compounds (from the biological assay) **3a**, **3f** and **3s** were docked with the active site of amino acids, where the hydrogen bonding interactions are shown by dotted lines (Figs. 2–4). The active site consisted of amino acid residue that bound to the corresponding amino acids such as ASN346, THR316, ALA318 and SER64. However, ASN346 was found to be conserved in the active site. The binding energy of ligand **3a** with protein active site was found to be −117.819 kcal mol^{-1}. The best pose for molecule **3s** shows two interactions with lowest energy of −113.067 kcal mol^{-1} which binds to the active site amino acids ASN346 and ARG148,

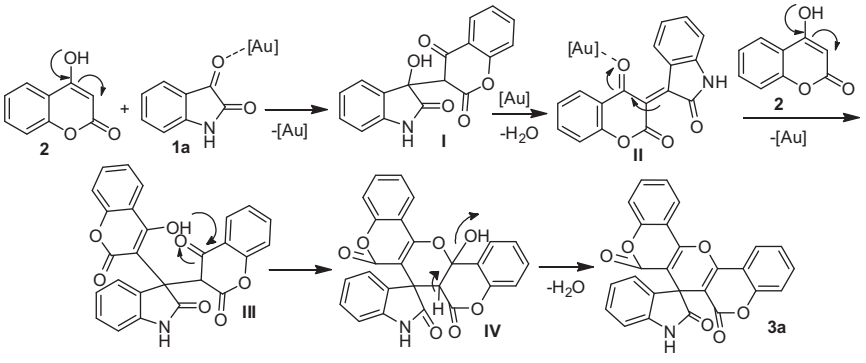

Scheme 5. Plausible mechanism for the formation of spirooxindole **3a**.

Table 3
Zone of inhibition (mm) of compounds **3a**–**3u** (1 mg/disc)

Compounds	Bacteria									Fungi	
	S. epidermidis	*S. typhimurium*	*K. pneumoniae*	*B. subtilis*	*S. flexneri*	*M. luteus*	*E. aerogenes*	*S. aureus*	*S. aureus* MRSA	*C. albicans*	*M. pachydermatis*
3a	**31**	**26**	**28**	**32**	**35**	**36**	**32**	**21**	**36**	**34**	**22**
3b	19	13	12	17	22	21	16	10	21	19	15
3c	21	16	17	21	23	20	18	11	23	23	20
3d	18	12	13	20	22	21	17	10	27	21	19
3e	**26**	**19**	**20**	**25**	**31**	**27**	**23**	**15**	**31**	**29**	**27**
3f	**31**	**24**	**26**	**31**	**35**	**30**	**29**	**24**	**38**	**36**	**23**
3g	17	15	12	11	13	11	11	12	12	12	13
3h	22	15	17	21	24	19	18	10	23	12	10
3i	17	12	13	16	19	18	15	10	20	14	15
3j	21	14	15	18	18	20	13	12	21	16	13
3k	**27**	**20**	**21**	**27**	**31**	**28**	**24**	**17**	**33**	**30**	**28**
3l	**28**	**19**	**22**	**29**	**33**	**23**	**23**	**15**	**32**	**29**	**30**
3m	12	11	13	12	11	11	13	12	14	14	12
3n	14	12	13	13	11	12	12	12	13	12	13
3o	13	15	12	16	11	11	15	10	12	12	13
3p	**30**	**22**	**25**	**29**	**34**	**29**	**24**	**16**	**33**	**32**	**29**
3q	13	11	15	12	12	12	13	11	16	14	13
3r	**26**	**19**	**21**	**25**	**30**	**27**	**22**	**15**	**31**	**33**	**26**
3s	**32**	**25**	**27**	**33**	**36**	**32**	**30**	**23**	**35**	**33**	**22**
3t	**25**	**18**	**21**	**26**	**30**	**27**	**23**	**15**	**30**	**31**	**27**
3u	20	14	11	19	16	12	21	13	17	18	14
Control	25	18	20	25	30	26	22	14	30	28	26

Control: streptomycin (standard antibacterial agent) and ketoconazole (standard antifungal agent).

Table 4
MIC of most potent compounds

Organism	**3a**	**3e**	**3f**	**3k**	**3l**	**3p**	**3r**	**3s**	**3t**	Control
Bacteria										
S. epidermidis	250	500	**31.25**	500	500	250	500	**31.25**	500	25
S. typhimurium	250	500	250	500	250	125	250	125	125	30
K. pneumoniae	250	500	61.25	500	500	500	125	250	250	6.25
B. subtilis	125	500	125	250	31.25	500	500	125	500	25
S. flexneri	61.25	500	250	500	250	500	125	125	125	6.25
M. luteus	250	500	125	500	61.25	250	500	125	500	6.25
E. aerogenes	**31.25**	250	125	250	500	250	500	125	500	25
S. aureus	250	500	**7.81**	250	125	250	250	**7.81**	61.25	6.25
S. aureus MRSA	**7.81**	500	125	250	500	250	500	250	250	6.25
Fungi										
C. albicans	250	500	500	250	500	250	250	**31.25**	250	25

Control: streptomycin (for antibacterial) and ketoconazole (for antifungal).

respectively. The best poses for molecule **3f** shows three interactions with lowest energy of −107.056 kcal mol^{-1} which binds to active site amino acids ASN346, GLU272 and ARG148, respectively. The docking study revealed that compound **3a** exhibited the minimum binding energy which indicates its strong affinity with the protein and has been stabilized by strong hydrogen bond interaction in the binding pocket.

Checkpoint kinase 1 (CHK1) is a protein kinase from the CAMKL kinase family, is a key element in the DNA damage response pathway and plays a crucial role in the S-G2-phase checkpoint.[18] Each phase of the cell cycle is regulated by several checkpoint mechanisms, such as DNA damage or spindle assembly checkpoints. First-line therapies for cancer include radiation and chemotherapy and are designed to induce cell death by damaging the DNA material of cancerous cells. Because cancer cells utilize the checkpoints to facilitate repair of their DNA, the inhibition of CHK1 represents an attractive strategy for sensitizing cancer cells to cytotoxic chemotherapeutics. To this end, all compounds were docked into the relative binding site of CHK1 crystal structures and the optimal conformations of these compounds were determined. To investigate the potential binding mode of inhibitors, all the compounds were subjected to molecular docking using the AutoDock 1.5.4 program. As a reference to other compounds, pyrazolo[1,5-*a*] pyrimidine was used as a model drug to show the binding modes of CHK1 inhibitors. From the docking scores, the free energy of binding (FEB) of all compounds were calculated (Table 5). The overlaid pose of bound and docked pyrazolo[1,5-*a*]pyrimidine ligand in the active site of CHK1 is shown in Figure 5. The results of which revealed that compound **3g** as the most active with a calculated binding energy of −8.99 kcal/mol and the least binding energy was exhibited by compound **3p** with a binding energy of −6.71 kcal/mol (Fig. 6). The binding interactions of other potent compounds exhibiting comparable IC_{50} and FEB values against the reference drugs such as **3a**, **3e**, **3f**, **3k**, **3l**, **3m**, **3n**, **3q**, **3s**, **3t** and **3u** were shown in the Supporting information.

To elucidate the interaction mechanism, the most potent inhibitors among the dataset, were selected for more detailed analysis. The ligand–enzyme interaction analysis shows that Leu137, Glu91, Cys87, Asp148, Ser88, Gly90 and Tyr86 are the important residues present in the active site. As shown in Figure 5, pyrazolo [1,5-*a*]pyrimidine binds to the kinase through key H-bond interactions: (i) between the –NH of cyclohexyl ring and the –COO of Glu91 (–O···HN, 1.90 Å, 160.9°); (ii) between the backbone carbonyl oxygen of Cys87 and the amino group of pyrimidine ring

Table 5
IC_{50} and FEB values of compounds **3a**–**3u**

Entry	Compounds	IC_{50} (μM)	FEB[a] (kcal/moL)
1	**3a**	57.2	−8.24
2	**3b**	>100	−7.01
3	**3c**	>100	−7.88
4	**3d**	>100	−7.77
5	**3e**	55.5	−7.99
6	**3f**	52.7	−8.77
7	**3g**	50.0	−8.99
8	**3h**	>100	−6.99
9	**3i**	>100	−7.75
10	**3j**	>100	−8.12
11	**3k**	54.5	−8.44
12	**3l**	53.9	−8.34
13	**3m**	51.1	−8.63
14	**3n**	51.8	−8.87
15	**3o**	>100	−7.58
16	**3p**	>100	−6.71
17	**3q**	54.2	−8.55
18	**3r**	>100	−7.74
19	**3s**	53.1	−8.31
20	**3t**	51.8	−8.44
21	**3u**	55.3	−8.33
22	Standard[b,c]	—	−9.53

[a] FEB = free energy of binding.
[b] Cyclophosphamide was used as the standard for cytotoxic studies, which showed 90% inhibition (156 μM).
[c] Pyrazolo[1,5-*a*]pyrimidine was used as the standard for docking.

(–O···HN, 2.46 Å, 129.8°; –O···HN, 3.47 Å, 150.2°); (iii) between the nitrogen atom of pyrazole ring and the -NH group of Cys87 residue (–N···HN, 2.37 Å, 157.6°); (iv) the interaction between the nitrogen atom of another pyrazole ring and the side chain of Asp148 is bridged by a structural molecule W502; (v) pyrazolo [1,5-*a*]pyrimidine ring forms arene-cation interaction with Leu137 which further enhances the binding activity. The docking results were well in consistent with the in vitro CHK1 inhibitory biological activity (IC_{50}). The specific cleft in which the compounds bind in the active site contains polar residues (Glu85, Tyr86, Cys87, Ser88, Gly89, Gly90, Glu91, Ser147 and Asp148) and non-polar residues (Ala36, Leu84 and Val23). The compounds **3a**, **3f**, **3g**, **3k**, **3l**, **3m**, **3n**, **3q** and **3u** are well placed inside the active site and demonstrate the following interactions. (i) The oxygen atom of spirooxindole forms H-bond with –NH group of Cys87 (–O···HN, 2.15 Å). (ii) The –NH group of indole ring forms H-bond with the backbone –CO of Glu85 (–O···HN, 1.95 Å). It is remarkable to note that the large spirooxindole moiety has sufficient room to get incorporated into the hydrophobic pocket composed by Ala36, Leu84 and Val23. The docking score was improved, when the R substituent was hydrogen, methyl, ethyl, propyl and butyl (**3a**, **3k**, **3l**, **3m** and **3n**). Interestingly, the CHK1 inhibitory activity also improved in the same way. The similar binding mode and docking score as well as CHK1 inhibitory activity was also observed in compounds **3f**, **3g**, **3q** and **3u**. The pentyl (**3o**) and hexyl (**3p**) groups were not able to accommodate into the active site, hence the docking score and CHK1 inhibitory activity also reduced. Ligands with bulky substituent like benzyl (**3s**) and 2-fluorobenzyl (**3t**) showed different binding mode on the same active site. The oxygen atom of indole ring forms H-bond with –NH group of Glu84 (–O···HN, 2.76 Å). The –NH group of indole ring forms H-bond with the backbone –CO of Glu85 (–O···HN, 2.15 Å). Based on the observations, we conclude that the network of H-bonds formed between CHK1 and the compounds are crucial for molecular recognition.

In summary, we have developed a protocol for the gold(III)-catalyzed bis-condensation reaction between isatins with 4-hydroxycoumarins. The reaction proceeds under microwave conditions, extends the substrate class to *N*-substituted isatins and bis-isatins to provide the corresponding spirooxindole products with up to 95% yield (22 examples). The developed methodology shows promising advantages such as high yielding, short reaction time and no requirement of tedious purification techniques. Antimicrobial screening of spirooxindole derivatives against a wide panel of antimicrobial strains showed that three compounds (**3a**, **3f** and **3s**) exhibited significant MIC values compared to the reference drugs. Docking with AmpC-β-lactamase receptor revealed that compound **3a** is the most active by exhibiting a minimum free energy of binding (–117.819 kcal/mol). All compounds were also evaluated for their cytotoxic potency against COLO320 cancer cells. The results of which indicated that compound **3g** exhibited significant inhibitory potency with IC_{50} values of 50.0 μM. Molecular docking with CHK1 receptor also supported the biological results by showing compound **3g** as the most active with a free energy of binding −8.99 kcal/mol. Our future studies will be directed towards the utilization of these structurally interesting heterocycles in the synthesis of improved chemical entities (ICE) and new drug discovery research.

Acknowledgements

The work has been financially supported by a fast track grant for young scientists (Grant no: SERB/F/5666/2015-16) from Science and Engineering Research Board (SERB), India. C.P. is grateful to Dr.

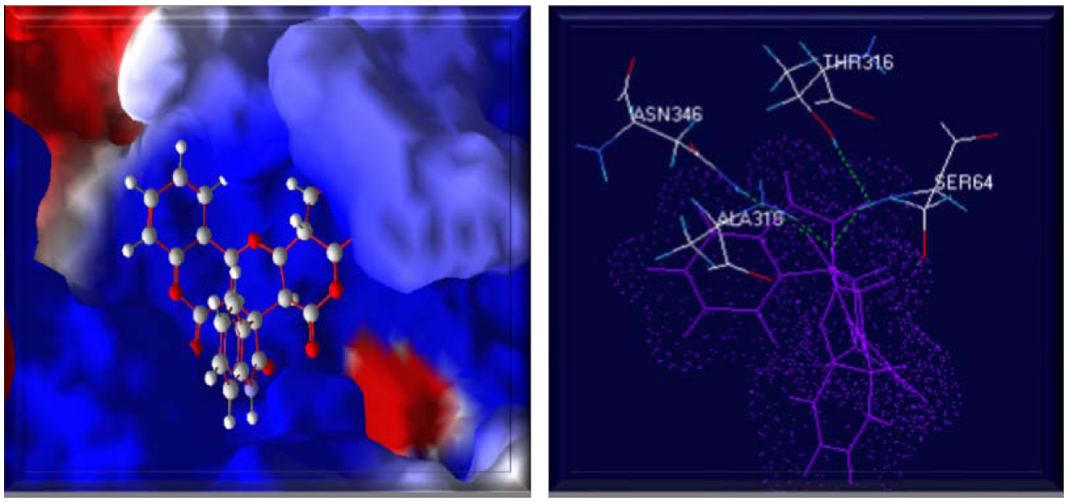

Figure 2. Putative binding pose of compound **3a** in AmpC-β-lactamase (left panel). Docking of compound **3a** in AmpC-β-lactamase, where hydrogen bonding interactions are shown in dotted lines (right panel).

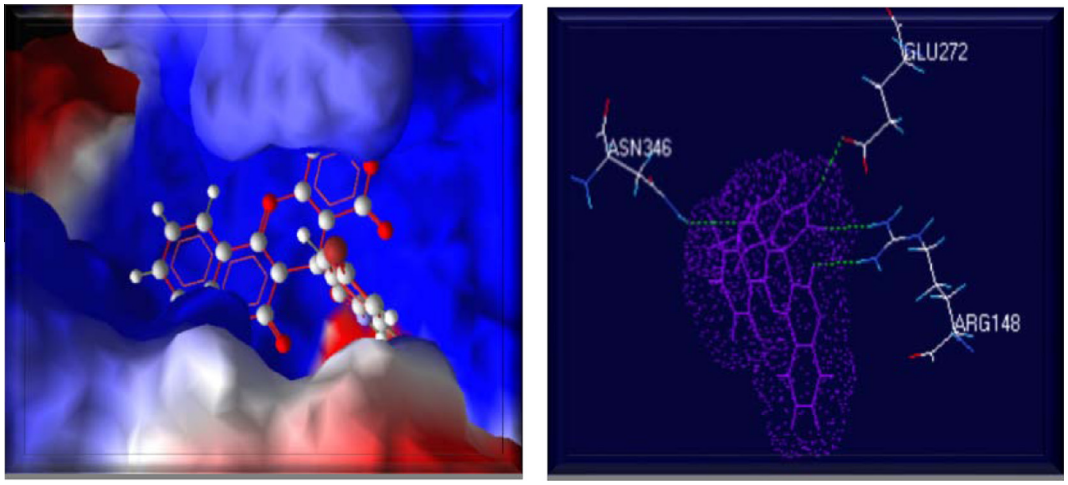

Figure 3. Putative binding pose of compound **3f** in AmpC-β-lactamase (left panel). Docking of compound **3f** in AmpC-β-lactamase, where hydrogen bonding interactions are shown in dotted lines (right panel).

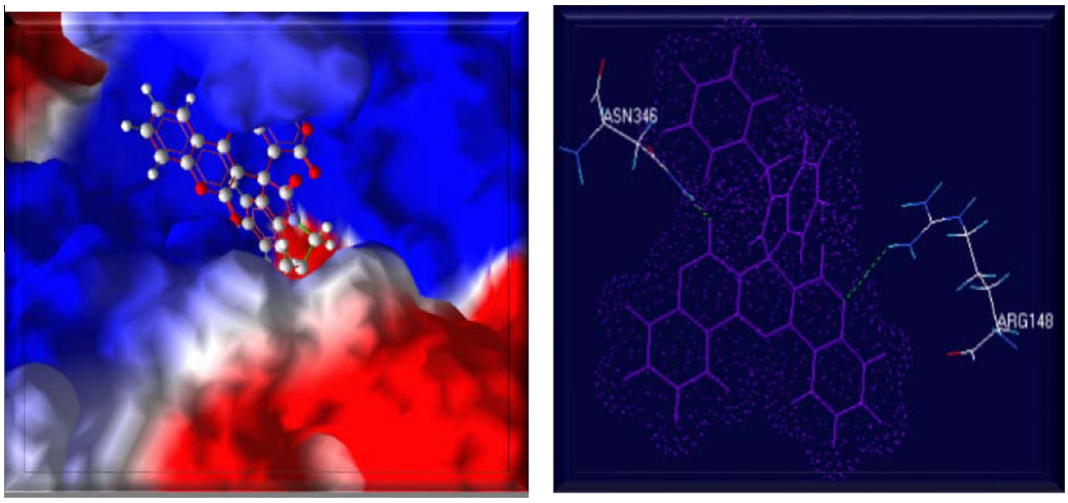

Figure 4. Putative binding pose of compound **3s** in AmpC-β-lactamase (left panel). Docking of compound **3s** in AmpC-β-lactamase, where hydrogen bonding interactions are shown in dotted lines (right panel).

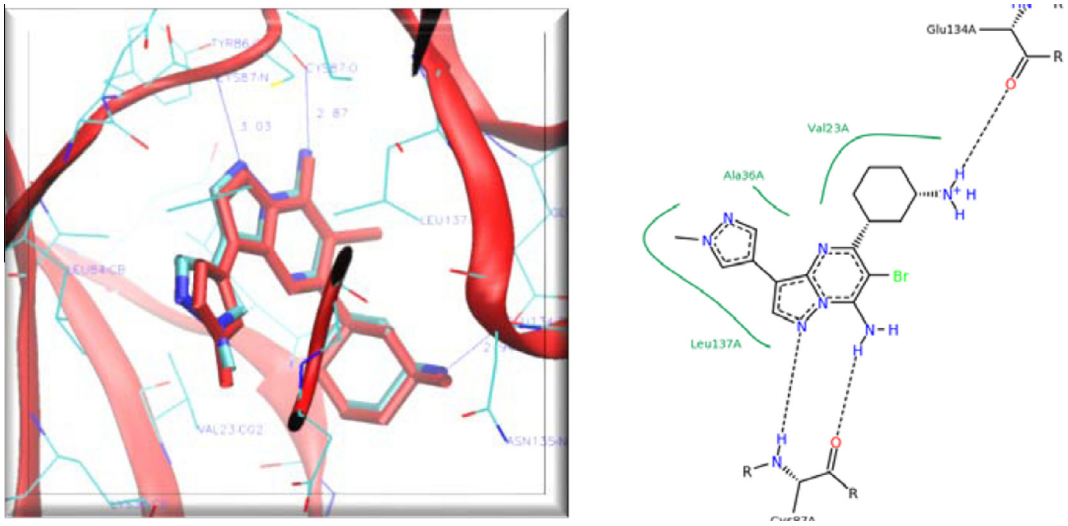

Figure 5. Overlaid pose of bound and docked co-crystal (left panel). Hydrogen bonding interactions of reference drug, pyrazolo[1,5-*a*]pyrimidine with CHK1 receptor.

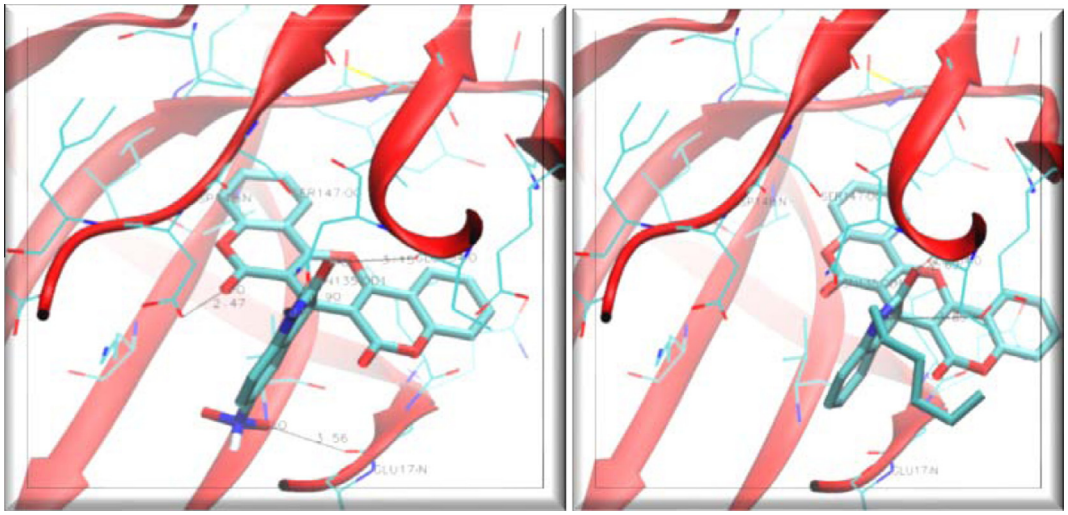

Figure 6. Docking pose of most active compound **3g** (left panel). Docking pose of least active compound **3p** (right panel).

Vijayamohanan K. Pillai, Director, CSIR-CECRI for allowing to publish this work and Dr. D. Jeyakumar, Head, Functional Materials Division, CSIR-CECRI for providing laboratory and analytical facilities.

Supplementary data

Experimental procedure for synthesis, antimicrobial evaluation, cytotoxicity and molecular docking studies are given in the supporting information. IR, ^{1}H NMR, ^{13}C NMR, mass spectra and molecular docking poses. Supplementary data associated with this article can be found, in the online version, at http://dx.doi.org/10.1016/j.bmcl.2016.07.036.

References and notes

1. (a) Williams, R. M.; Cox, R. J. *Acc. Chem. Res.* **2003**, *36*, 127; (b) da Silva, J. F. M.; Garden, S. J.; Pinto, A. C. *J. Braz. Chem. Soc.* **2001**, *12*, 273; (c) Tang, Y. Q.; Sattler, I.; Thiericke, R.; Grabley, S.; Feng, X. Z. *Eur. J. Org. Chem.* **2001**, 261; (d) Tsuda, M.; Mugishima, T.; Komatzu, K.; Sone, T.; Tanaka, M.; Mikami, Y.; Shiro, M.; Hirai, M.; Ohizumii, Y.; Kobayashi, J. *Tetrahedron* **2003**, *59*, 3227; (e) Jossang, A.; Jossang, P.; Hadi, H. A.; Sevenet, T.; Bodo, B. *J. Org. Chem.* **1991**, *56*, 6527; (f) James, M. N. G.; Williams, G. J. B. *Can. J. Chem.* **1972**, *50*, 2407; (g) Elderfield, R. C.; Gilman, R. E. *Phytochemistry* **1972**, *11*, 339; (h) Wang, L.; Zhang, Y.; Hu, H.-Y.; Fun, H. K.; Xu, J.-H. *J. Org. Chem.* **2005**, *70*, 3850; (i) Cui, C. B.; Kakeya, H.; Okada, G.; Onose, R.; Osada, H. *J. Antibiot.* **1996**, *49*, 527.
2. (a) Beinema, M.; Brouwers, J. R.; Schalekamp, T.; Wilffert, B. *Thromb. Haemost.* **2008**, *100*, 1052; (b) Shi, Y.; Zhou, C.-H. *Bioorg. Med. Chem. Lett.* **2011**, *21*, 956; (c) Khodabakhshi, S.; Karami, B.; Eskandari, K.; Hoseini, S. J.; Rashidi, A. *RSC Adv.* **2014**, *4*, 17891; (d) Au, N.; Rettie, A. E. *Drug. Metab. Rev.* **2008**, *40*, 355.
3. (a) Gao, L.; Zha, Y.; Tao, S.; Gao, Y.; Chen, M.; Jiang, L.; Rong, L. *Res. Chem. Intermed.* **2015**, *41*, 5627; (b) Almansour, A. I.; Kumar, R. S.; Arumugam, N.; Shree, P. D.; Suresh, J. *Acta Crystallogr.* **2012**, *E68*, o744; (c) Almansour, A. I.; Kumar, R. S.; Arumugam, N.; Vishnupriya, R.; Suresh, J. *Acta Crystallogr.* **2012**, *E68*, o1194; (d) Almansour, A. I.; Kumar, R. S.; Arumugam, N.; Kanagalaksmi, S.; Suresh, J. *Acta Crystallogr.* **2012**, *E68*, o1172.
4. (a) Jain, S. C.; Talwar, S.; Bhagat, S.; Rajwanshi, V. K.; Kumar, R.; Babu, B. R. *Pure Appl. Chem.* **1996**, *68*, 739; (b) Jain, S. C.; Bhagat, S.; Rajwanshi, V. K.; Babu, B. R.; Sinha, J. *Ind. J. Chem.* **1997**, *36B*, 633.
5. (a) Jeyaveeran, J. C.; Praveen, C.; Arun, Y.; Prince, A. A. M.; Perumal, P. T. *J. Chem. Sci.* **2016**, *128*, 73; (b) Praveen, C.; Perumal, P. T. *Chin. J. Catal.* **2016**, *37*, 288; (c) Praveen, C.; Perumal, P. T. *Synthesis* **2016**, *48*, 855; (d) Jeyaveeran, J. C.; Praveen, C.; Arun, Y.; Prince, A. A. M.; Perumal, P. T. *J. Chem. Sci.* **2016**, *128*, 787; (e) Praveen, C.; Ananth, D. B. *Bioorg. Med. Chem. Lett.* **2016**, *26*, 2507; (f) Praveen, C.; Kiruthiga, P.; Perumal, P. T. *Synlett* **2009**, 1990; (g) Praveen, C.; Jegatheesan, S.; Perumal, P. T. *Synlett* **2009**, 2795; (h) Praveen, C.; Kalyanasundaram, A.; Perumal, P. T. *Synlett* **2010**, 777; (i) Praveen, C.; Sagayaraj, Y. W.; Perumal, P. T. *Tetrahedron Lett.* **2009**, *50*, 644; (j) Praveen, C.; Karthikeyan, K.; Perumal, P. T. *Tetrahedron* **2009**, *65*, 9244; (k) Praveen, C.; Perumal, P. T. *Synlett* **2011**, 521; (l) Praveen, ; Ayyanar, A.; Perumal, P. T. *Bioorg. Med. Chem. Lett.* **2011**, *21*, 4170.
6. (a) Galema, S. A. *Chem. Soc. Rev.* **1997**, *26*, 233; (b) Rajak, H.; Mishra, P. *J. Sci. Ind. Res.* **2004**, *63*, 641.
7. (a) Shmidt, M. S.; Perillo, I. A.; González, M.; Blanco, M. M. *Tetrahedron Lett.* **2012**, *53*, 2514; (b) Chen, G.; Liu, B.; Tang, Y.; Deng, Q.; Hao, X.-J. *Heterocycl. Commun.* **2010**, *16*, 25; (c) Diaz, P.; Xu, J.; Astruc-Diaz, F.; Pan, H.-M.; Brown, D. L.; Naguib, M. *J. Med. Chem.* **2008**, *51*, 4932; (d) Bacchi, A.; Carcelli, M.; Pelagatti, P.; Pelizzi, G.; Rodriguez-Arguelles, M. C.; Rogolino, D.; Solinas, C.; Zani, F. *J. Inorg. Biochem.* **2005**, *99*, 397; (e) Chowdhury, S.; Liu, S.; Cadieux, J. A.; Hsieh, T.; Chafeev, M.; Sun, S.; Jia, Q.; Sun, J.; Wood, M.; Langille, J.; Sviridov, S.; Fu, J.; Zhang, Z.; Chui, R.; Wang, A.; Cheng, X.; Zhong, J.; Hossain, S.; Khakh, K.; Rajlic, I.; Verschoof, H.; Kwan, R.; Young, W. *Med. Chem. Res.* **2013**, *22*, 1825; (f) Shi, F.; Tao, Z.-L.; Luo, S.-W.; Tu, S.-J.; Gong, L.-Z. *Chem. Eur. J.* **2012**, *18*, 6885; (g) Sharma, R.; Pandey, A. K.; Shivahare, R.; Srivastava, K.; Gupta, S.; Chauhan, P. M. S. *Bioorg. Med. Chem. Lett.* **2014**, *24*, 298; (h) Shakoori, A.; Bremner, J. B.; Willis, A. C.; Haritakun, R.; Keller, P. A. *J. Org. Chem.* **2013**, *78*, 7639; (i) Rassu, G.; Zambrano, V.; Tanca, R.; Sartori, A.; Battistini, L.; Zanardi, F.; Curti, C.; Casiraghi, G. *Eur. J. Org. Chem.* **2012**, 466; (j) Vintonyak, V. V.; Warburg, K.; Over, B.; Hübel, K.; Rauh, D.; Waldmann, H. *Tetrahedron* **2011**, *67*, 6713; (k) Wee, X. K.; Yang, T.; Go, M. L. *ChemMedChem* **2012**, *7*, 777; (l) Rahmati, A.; Khalesi, Z. *Tetrahedron* **2012**, *68*, 8472.
8. (a) Fürstner, A.; Davies, P. W. *Angew. Chem., Int. Ed.* **2007**, *46*, 3410; (b) Núñez, E. J.; Echavarren, A. M. *Chem. Commun.* **2007**, 333.
9. (a) Nandi, B.; Kundu, N. G. *J. Chem. Soc., Perkin Trans. 1* **2001**, 1649; (b) Fortes, C. C.; Garrote, C. F. D. *Synth. Commun.* **1997**, *27*, 3917; (c) Noguchi, M.; Okada, M. H.; Watanabe, M.; Okuda, K.; Nakamura, O. *Tetrahedron* **1996**, *52*, 6581; (d) Abbiati, G.; Canevari, V.; Caimi, S.; Rossi, E. *Tetrahedron Lett.* **2005**, *46*, 7117.
10. Liang, B.; Kalidnidi, S.; Porco, J. A., Jr.; Stephenson, C. R. J. *Org. Lett.* **2010**, *12*, 572.
11. (a) Praveen, C.; Narendiran, S.; Dheenkumar, P.; Perumal, P. T. *J. Chem. Sci.* **2013**, *125*, 1543; (b) Praveen, C.; Iyyappan, C.; Girija, K.; Kumar, K. S.; Perumal, P. T. *J. Chem. Sci.* **2012**, *124*, 451; (c) Praveen, C.; Ayyanar, A.; Perumal, P. T. *Bioorg. Med. Chem. Lett.* **2011**, *21*, 4072; (d) Praveen, C.; Dheenkumar, P.; Muralidharan, D.; Perumal, P. T. *Bioorg. Med. Chem. Lett.* **2010**, *20*, 7292; (e) Parthasarathy, K.; Praveen, C.; Balachandran, C.; Kumar, P. S.; Ignacimuthu, S.; Perumal, P. T. *Bioorg. Med. Chem. Lett.* **2013**, *23*, 2708; (f) Parthasarathy, K.; Praveen, C.; Kumar, P. S.; Balachandran, C.; Perumal, P. T. *RSC Adv.* **2015**, *5*, 15818; (g) Praveen, C.; Nandakumar, A.; Dheenkumar, P.; Muralidharan, D.; Perumal, P. T. *J. Chem. Sci.* **2012**, *124*, 609.
12. Bauer, A. W.; Kirby, W. M.; Sherris, J. C.; Turck, M. *Am. J. Clin. Pathol.* **1996**, *45*, 493.
13. (a) Candan, F.; Unlu, M.; Tepe, B.; Daferera, D. M.; Polissiou, M.; Sökmen, A.; Akpulat, H. A. *J. Ethnopharmacol.* **2003**, *87*, 215; (b) Duraipandiyan, V.; Ignacimuthi, V. *J. Ethnopharmacol.* **2009**, *123*, 494.
14. (a) Mossman, T. *J. Immunol. Methods* **1983**, *65*, 55; (b) Wallace, A. C.; Lasowski, R. A.; Thornton, J. M. *Protein Eng.* **1995**, *8*, 127; (c) Alley, M. C.; Scudiero, D. A.; Monks, A.; Hursey, M. L.; Czerwinski, M. J.; Fine, D. L.; Abbott, J. G. M.; Shoemaker, R. H.; Boyd, M. R. *Cancer Res.* **1988**, *48*, 589; (d) Slater, T. F.; Sawyer, B.; Sträuli, U. *Biochem. Biophys. Acta* **1963**, *77*, 383.
15. (a) Taylor, R. D.; Jewsbury, P. J.; Essex, J. W. *J. Comput. Aid. Mol. Des.* **2002**, *16*, 151; (b) Gohlke, H.; Klebe, G. *Curr. Opin. Struct. Biol.* **2001**, *11*, 231.
16. Vanderpool, D.; Johnson, T. O.; Ping, C.; Bergqvist, S.; Alton, G.; Phonephaly, S.; Rui, E.; Luo, C.; Deng, Y.-L.; Grant, S.; Quenzer, T.; Margosiak, S.; Register, J.; Brown, E.; Ermolieff, J. *Biochemistry* **2009**, *48*, 9823.
17. Powers, R. A.; Shoichet, B. K. *J. Med. Chem.* **2002**, *45*, 3222.
18. Labroli, M.; Paruch, K.; Dwyer, M. P.; Alvarez, C.; Keertikar, K.; Poker, C.; Rossman, R.; Duca, J. S.; Fischmann, T. O.; Madison, V.; Parry, D.; Davis, N.; Seghezzi, W.; Wiswell, D.; Guzi, T. J. *Bioorg. Med. Chem. Lett.* **2011**, *21*, 471.